Effective elastic moduli of space-filled multi-material composite lattices

T. Mukhopadhyay[1,*], S. Naskar[1], D. Kundu[2], S. Adhikari[3]

[1] *Faculty of Engineering and Physical Sciences, University of Southampton, Southampton SO17 1BJ, UK*
[2] *Department of Aerospace Engineering, Indian Institute of Technology Kanpur, Kanpur, India*
[3] *James Watt School of Engineering, University of Glasgow, Glasgow G12 8QQ, UK*
[*] *Email address: T.Mukhopadhyay@soton.ac.uk*

Abstract

Traditionally lattice materials are made of a network of beams in two and three dimensions with majority of the lattice volume being void space. Recently researchers have started exploring ways to exploit this void space for multi-physical property modulation of lattices such as global mechanical behaviour including different elastic moduli, wave propagation, vibration, impact and acoustic features. The elastic moduli are of crucial importance to ensure the structural viability of various multi-functional devices and systems where a space-filled lattice material could potentially be used. Here we develop closed-form analytical expressions for the effective elastic moduli of space- filled lattices based on an exact stiffness matrix approach coupled with the unit cell method, wherein transcendental shape functions are used to obtain exact solutions of the underlying differential equation. This can be viewed as an accurate multi-material based generalization of the classical formulae for elastic moduli of honeycombs. Numerical results show that the effective in-plane elastic moduli can increase by orders of magnitude with a relatively lower infill stiffness ($\sim$10%).This gives an exceptional opportunity to engineer multi-material lattices with optimal specific stiffness along with characterizing the mechanical properties of a multitude of lattice-like artificial and naturally occurring structural forms with space filling.

Keywords: Hexagonal lattice; Effective elastic moduli; Space-filled lattice metamaterials; Multi-material honeycombs; Composite lattices

Contents

1. Introduction

Two and three dimensional lattice-like periodic microstructures provide an unprecedented opportunity to artificially engineer the global (i.e. effective) mechanical properties of materials based

on multi-functional bespoke demands of modern structural systems by identifying (or designing) the intrinsic material and micro-scale structural topology. Mechanical properties of lattice-like honeycomb structures have received tremendous attention from the scientific community over the last few decades. Traditionally such lattices are made of a network of beams in two and three dimensions with majority of the volume of the lattice structure being void space. Recently researchers have started exploring ways to exploit this void space for multi-functional property modulation of lattices. For example, if we could have a filled multi-material lattice structure, the global mechanical behaviour including different elastic moduli, wave propagation, vibration, impact and acoustic features can be simultaneously modulated in a substantially expanded design space with additional parameters related to the stiffness, mass and damping of the filler, leading to exciting multi-functional properties. It may be noted that the elastic moduli are always of crucial importance to ensure the structural viability of various multi-functional devices and systems where a space-filled lattice material could potentially be used. In this article, we aim to develop efficient analytical expressions for the effective in-plane elastic moduli of such space-filled lattices. An explicit theoretical characterization of the elastic properties along with necessary physical insights underpinning the configuration space of multi-material and geometric parameters will accelerate potential exploitation of filled lattices in various engineered multi-functional materials and structures across different length-scales with advantage of an expanded design space.

In microstructured lattice materials the tailorable effective macro-scale mechanical properties (such as equivalent elastic moduli, deformation, stability, energy absorption, vibration, energy harvesting, impact and wave propagation characteristics with programmable features) are defined by the microstructural geometric configuration along with the intrinsic material properties of constituent members. Naturally occurring monolithic materials cannot exhibit one or more of the fascinating multi-functional properties like negative Poisson's ratio, extremely lightweight characteristics, negative stiffness, pentamode material characteristics (meta-fluid) and a weighted combination of various such unusual (or usual) properties, which can effectively be obtained by intelligent and intuitive microstructural designs [1, 2, 3, 4, 5, 6, 7]. For example, the conventional positive effective Poisson's ratio (which is usually exhibited by normal materials) in hexagonal lattice microstructures can be converted to negative, or zero by intuitively designing the hexagonal unit cell [8, 9], as depicted in figure 1(E-G). Besides static properties [10], various unusual yet critically useful effective properties can be realized in engineered microstructures under dynamic condition, such as negative bulk modulus [11], negative mass density [12], negative Young's modulus [13], negative shear modulus [14], band structure modulation [15] and elastic cloaks [16]. Computational homogenization has been widely adopted to report the effective lattice-level properties of metamaterials [17, 18, 19, 20, 21, 22, 23]. Recent developments in this filed include active and on-demand programming of effective elastic properties by exploiting stimuli-sensitive intrinsic materials [24, 25]. These novel class of artificially engineered metamaterials with tailorable and programmable macroscale properties have extraordinary potential for applications in advanced and futuristic multi-functional engineering systems.

Normally two material properties (or more, in case of multi-material lattices) are involved at two widely apart length-scales in lattice metamaterials. One is the intrinsic material(s) (more than one such material may be involved in multi-material microstructural topologies) which is actually the material of the constituting elements (such as the connecting beam or cell wall members shown in figure 1(D)) at micro-scale. Materials at this relatively lower length scale (often referred as the microscale) are either monolithic materials or different alloys and compounds. The chemical composition, atomic and molecular structure of these intrinsic materials decide the mechanical properties at this length scale. The second set of material properties (at a relatively much higher length scale) correspond to the effective macro-scale homogenized behaviour of the entire lattice. Such macro-scale properties depend on the intrinsic lower-scale (micro) material properties and the lower scale microstructural topology (microstructural geometry) of the lattice. The compound effect of these two factors leads to a tremendous opportunity of achieving unprecedented effective mechanical and multi-physical properties that are not exhibited by conventional

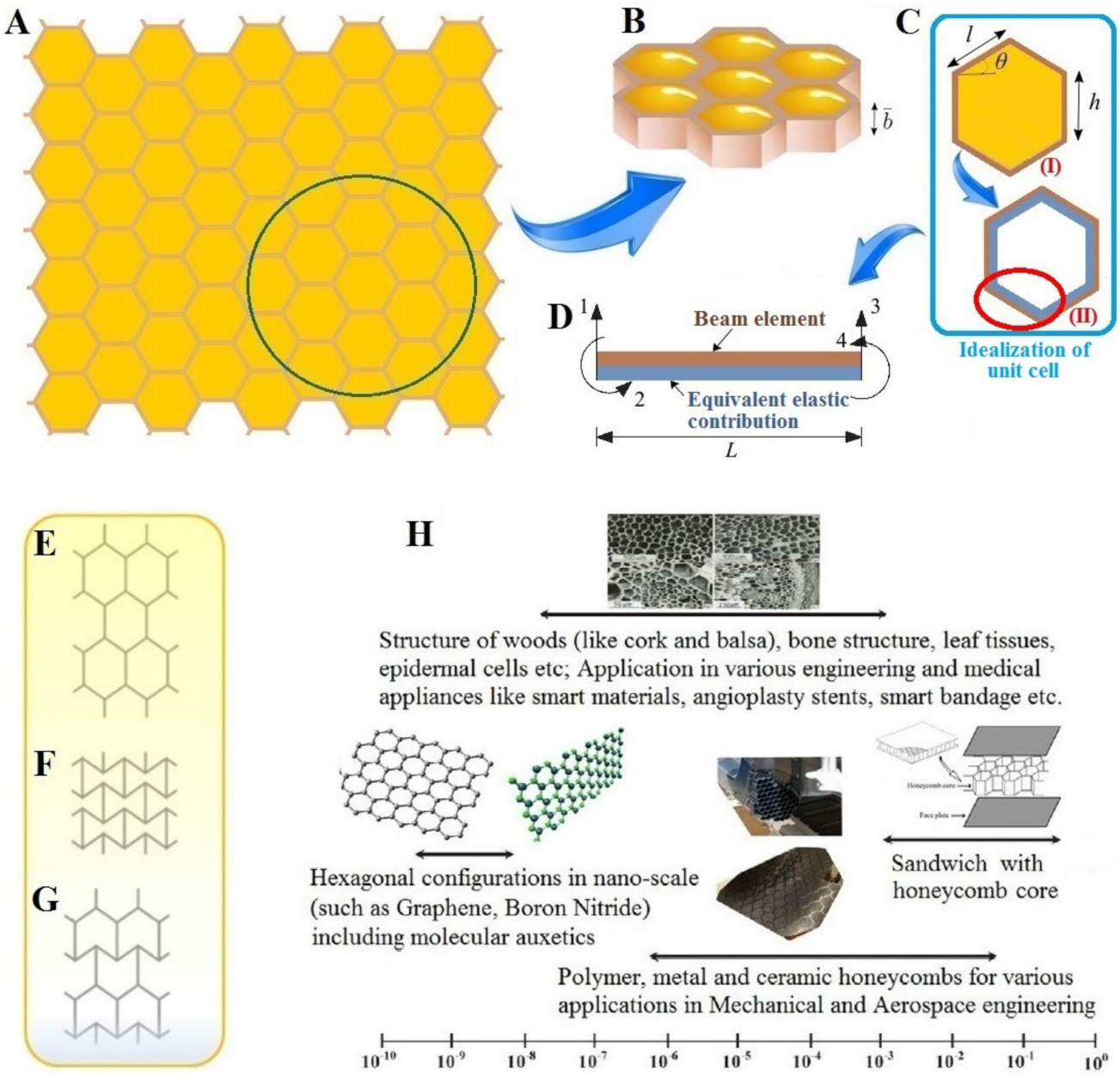

Figure 1: Microstructural details of space-filled honeycombs. (A) Typical representation of a hexagonal filled honeycomb structure. Two materials (materials of the honeycomb cell walls and the filler) involved in the periodic lattice are indicated using different colours. **(B)** Three dimensional view of the space-filled multi-material lattice structure. **(C)** Unit cell of the periodic structure along with microstructural geometry. Here we show both the actual unit cell and the idealized unit cell. The figure C(I) shows the actual unit cell with filler material. The idealized unit cell, which is used in the current analysis, is shown in figure C(II). In this idealized unit cell, effect of the filler material is replaced by an equivalent elastic contribution. **(D)** Typical representation of a general beam element of length L where each node has two degrees of freedom. The idealisation of the effect of filler material on the cell walls (i.e. the beam) is shown using the equivalent elastic contribution along the length of the beam. **(E-G)** The concept of modulating Poisson's ratio based on intuitive design of microstructural geometry (primarily, cell angle θ). Three typical microstructures are shown here that can exhibit positive (E), negative (F) and zero (G) Poisson's ratios. **(H)** Presence of hexagonal lattice structures across the length-scales (nano to macro) in natural and artificial systems. This shows the significance of analysing such lattices for new material development as well as characterization of existing materials and structural systems.

engineering materials. Though aperiodic, quasi-periodic and random microstructural topologies have been proposed, periodic lattice-like forms are predominant in the literature of metamaterials [26, 33]. A unit cell (analogous to representative volume element) based approach is adopted to model periodic microstructures with appropriate boundary conditions leading to a set of effective elastic moduli at macro-scale such that the lattice can be considered as an equivalent continuum [27, 28, 29, 30, 31, 32]. Edge effects [34] can be neglected in the such a unit cell based approach of

evaluating the effective elastic properties with the assumption of a substantially high number of cells. It is a valid assumption in the design of lattice materials and widely followed in the literature for obtaining equivalent global properties such as effective elastic moduli [28].

The fundamental mechanics for lattices (derived based on the unit cells with periodic boundary condition) being normally scale-independent, the scientific developments concerning the mechanics of deformation are applicable (directly or indirectly) to a broad range of periodic structural forms across nano to micro and macro scales. 2D lattices of hexagonal form are found across nano to micro and macro scales in various natural and artificial systems abundantly [33, 35, 36, 37], as depicted in figure 1(H). Moreover, hexagonal lattices can effectively be altered to rectangular, rhombic and auxetic configurations by taking the geometric parameters appropriately. Such widespread relevance and applicability of hexagonal lattices have motivated our current focus on this form of microstructure while adopting a lattice geometry to explain the concept of space-filling (including analytical derivation and numerical results). Though we would focus here on hexagonal lattices, the basic concepts and approach of analytical derivation are generic and they would be readily applicable (or extendable, albeit with different forms of final closed-form expressions) to various other 2D and 3D lattice geometries.

Most research activities for the development of mechanical metamaterials concentrate on the microstructural topologies for modulation of mechanical and multi-physical properties, rather than the intrinsic materials at the lower length-scale. Thus, one single material that is suitable for manufacturing and has adequate physical properties according to the intended application, is traditionally chosen as the constituent intrinsic material [38]. However, the recent tremendous advancements in manufacturing microstructures with multi-material configurations based on additive manufacturing [39, 40, 41] have created a strong rationale for developing a new class of metamaterial, where two or more intrinsic materials at the lower scale could be adopted to form the unit cell. Such multi-material lattices would expand the scope of multi-functional design significantly. Majority of the research related to multi-functional metamaterials adopt inverse design approach to identify the volume fractions of two or more intrinsic materials based on numerical algorithms [42, 43]. Multi-material lattice microstructures have shown exceptional promise for achieving unusual multi-physical properties like zero and negative thermal expansion coefficient along with modulation of other mechanical properties [44, 45]. The current focus of space-filled lattices is a special kind of multi-material periodic topology, where the intention is to exploit the void space in traditional lattices for enriching multifunctional properties. In principle, multimaterial topologies could have two different configurations for developing metamaterials. In the first microstructural configuration, the periodic unit cell have multiple intrinsic materials and the unit cell is tessellated in the 2D (or 3D) space to form a lattice. In the second configuration, the lattice is formed using two or more unit cells with different intrinsic material properties. The conventional unit cell approach can not be adopted for analyzing the second form of multi-material lattice as it may not lead to a truly periodic microstructure. The periodicity can remain unaltered (and subsequently a unit cell based approach is applicable) in the first form of multi-material lattice, which is the central focus of the current investigation.

We aim to investigate the effect of space-filling on the elastic moduli of honeycomb lattices with the notion of possible exploitation of the void space for multi-functional property augmentation. Elastic moduli of space-filled lattice structures are of quite practical relevance, such as foam-filled honeycombs applied in various sandwich panels. Moreover, the biological systems which adopt a hexagonal lattice-like structure at micro-scale are often found to be filled with fluids, fibres or other bulk materials. In these systems, the inner space-filling or foam-like core (with much lesser effective elastic moduli than the celle walls) behaves like an equivalent elastic contribution throughout the length of honeycomb cell walls, as depicted in figure 1(C-D). We would develop analytical expressions for the effective in-plane elastic moduli of space-filled lattices based on an exact element stiffness matrix approach coupled with the unit cell method, wherein transcendental shape functions would be used to satisfy the equilibrium at all points of the structural domain. For establishing the analytical model, the mechanical equivalence of space-filled lattices as equivalent

network of beams under the presence of the equivalent elastic contribution of the filler material will be utilised. The results would be compared to the effective elastic moduli obtained from the traditional stiffness matrices of beam elements with the equivalent elastic contribution of filler material. Further, separate finite element simulations would be carried out to validate the analytical expressions for space-filled lattices.

In the following sections we systematically present the derivation for elastic moduli of space-filled lattices based on the stiffness matrix of a beam element with the equivalent elastic contribution of filler material. Two different methods are followed for deriving the stiffness matrix of individual beam elements based on transcendental shape functions and conventional shape functions. Subsequent sections present numerical quantification to demonstrate the effect of space filling on the elastic moduli, followed by perspective and concluding remarks.

2. Mechanics of space-filled lattices

Deformation of the overall lattice microstructure depends on the mechanical behaviour of individual beams which make up the tessellating hexagonal unit cells (refer to figure 1(A-D))). Due to the elastic filling, each beam can be assumed to be acted upon by an equivalent elastic contribution of the filler material. A pictorial depiction of the beam along with the degrees of freedom at each node is provided in figure 1(D). Here our workflow is first to obtain the stiffness matrix of such a beam element (with equivalent contribution of filler) following two different approaches. Once this local beam-level property is obtained, a unit cell-based homogenisation will be employed to characterize the global elastic properties of the entire space-filled lattice.

In this context it can be noted that the determination of the equivalent filler modulus (as presented by k in the subsequent derivations) is an important aspect. Two cases may arise concerning the forward and inverse problems of space-filled lattices. (a) For designing novel space-filled bi-material lattices (inverse problem), the elastic properties of both the stiffer honeycomb cell walls and less-stiff filler material (i.e. the two intrinsic materials) can be evaluated based on conventional mechanical testing of bulk samples of the respective materials. (b) In case of characterizing the effective elastic properties of naturally occurring and artificial lattice structures with space-filling (forward problem), the individual elastic properties of the cell wall and filler material should be known a priori. For various mechanical systems such as foam-filled honeycombs, it is quite straightforward to evaluate the elastic properties of the two constituent intrinsic materials. However, it would involve advanced experimental techniques to characterize the intrinsic material properties at lower length scales such as space-filled micro-lattices in various biological systems.

2.1. Element stiffness matrices

The governing equation of transverse deflection $V(x)$ of a beam can be expressed as

$$EI\frac{d^4V(x)}{dx^4} + kV(x) = f(x) \tag{1}$$

Refer to the supplementary material (section S1.1) for further details on the above differential equation. Based on Equation 1, stiffness matrix of an equivalent beam element with the contribution from elastic filler material is derived here following two different approaches: conventional element stiffness matrix approach and exact element stiffness matrix approach (the accuracy of these two approaches would be discussed at a later stage of this manuscript). We assume that the beams under consideration follow the Euler-Bernoulli hypotheses and the elastic infill is modelled as an equivalent elastic contribution of the filler material throughout the beam length [46]. The conventional element stiffness matrix of a beam with equivalent elastic contribution of the filler material can be obtained as (refer to the supplementary material section S1.1 for detailed

derivation)

$$\begin{aligned}\mathbf{K}_e &= EI\int_0^L \frac{d^2\mathbf{N}(x)}{dx^2}\frac{d^2\mathbf{N}^T(x)}{dx^2}\mathrm{d}x + k\int_0^L \mathbf{N}(x)\mathbf{N}^T(x)\mathrm{d}x \\ &= \frac{EI}{L^3}\begin{bmatrix} 12 & 6L & -12 & 6L \\ 6L & 4L^2 & -6L & 2L^2 \\ -12 & -6L & 12 & -6L^2 \\ 6L & 2L^2 & -6L & 4L^2 \end{bmatrix} + \frac{kL}{420}\begin{bmatrix} 156 & 22L & 54 & -13L \\ 22L & 4L^2 & 13L & -3L^2 \\ 54 & 13L & 156 & -22L \\ -13L & -3L^2 & -22L & 4L^2 \end{bmatrix}\end{aligned} \tag{2}$$

Here L is the length of the beam element (i.e. cell wall of the honeycomb). E represents intrinsic Young's modulus of the cell wall members and k is the equivalent filler modulus. I represents the second moment of area for in-plane bending of the cell walls. For the special case when there is no elastic filler material (i.e. $k = 0$), the stiffness matrix derived above approaches to the classical stiffness matrix of a beam [47, 48].

The exact element stiffness matrix of an individual beam element with equivalent elastic contribution of the filler material can be given by the following closed-form expression (refer to the supplementary material section S1.2 for detailed derivation)

$$\mathbf{D}_e = \frac{2EIb}{(S^2-s^2)}\begin{bmatrix} 2\,b^2\,(SC+sc) & b\,(C^2-c^2) & -2\,b^2\,(cS+sC) & 2\,sSb \\ b\,(C^2-c^2) & SC-sc & -2\,sSb & sC-cS \\ -2\,b^2\,(cS+sC) & -2\,sSb & 2\,b^2\,(SC+sc) & -b\,(C^2-c^2) \\ 2\,sSb & sC-cS & -b\,(C^2-c^2) & SC-sc \end{bmatrix} \tag{3}$$

Elements of $\mathbf{D}_e$ are transcendental functions of (bL), where $C = \cosh(bL), c = \cos(bL), S = \sinh(bL), s = \sin(bL)$ and $b = \sqrt[4]{\frac{k}{4EI}}$ (refer to the supplementary material for further details).

The conventional stiffness matrix given in equation (2) appears to look different from the exact transcendental stiffness matrix in equation (3). To understand the nature of this visible difference, each element of the transcendental stiffness matrix is expanded in a Taylor series about $k = 0$. Substituting the expression of b in equation (3) and differentiating all the elements with respect to k, after simplifications we have the series expansion form

$$\begin{aligned}\mathbf{D}_e = {} & \frac{EI}{L^3}\begin{bmatrix} 12 & 6L & -12 & 6L \\ 6L & 4L^2 & -6L & 2L^2 \\ -12 & -6L & 12 & -6L^2 \\ 6L & 2L^2 & -6L & 4L^2 \end{bmatrix} + \frac{L}{420}\begin{bmatrix} 156 & 22L & 54 & -13L \\ 22L & 4L^2 & 13L & -3L^2 \\ 54 & 13L & 156 & -22L \\ -13L & -3L^2 & -22L & 4L^2 \end{bmatrix} k \\ & + \frac{L^5}{69854400EI}\begin{bmatrix} -25488 & -5352\,L & -23022 & 5043\,L \\ -5352\,L & -1136\,L^2 & -5043\,L & 1097\,L^2 \\ -23022 & -5043\,L & -25488 & 5352\,L \\ 5043\,L & 1097\,L^2 & 5352\,L & -1136\,L^2 \end{bmatrix} k^2 \\ & + \frac{L^9}{762810048000EI^2}\begin{bmatrix} 28960 & 113504\,L & 522090 & -112631\,L \\ 113504\,L & 24384\,L^2 & 112631\,L & -24273\,L^2 \\ 522090 & 112631\,L & 528960 & -113504\,L \\ -112631\,L & -24273\,L^2 & -113504\,L & 24384\,L^2 \end{bmatrix} k^3 + O(k^4) + \cdots\end{aligned} \tag{4}$$

It is interesting to note that the first two terms of this expansion are exactly the same as the conventional stiffness matrix in equation (2). The higher-order terms 'included' in the transcendental stiffness matrix account for the effect of elastic filler in an exact manner. Use of the conventional stiffness matrix would, therefore, be inaccurate for higher values of filler stiffness k unless the length of an element is made smaller. This fact gives rise to the significant advantage of using the transcendental stiffness matrix in the context of cellular lattice structures. We can use only one 'element' to represent the exact mechanical behaviour of the constituent parts of a unit cell. As no discretisation is necessary, it is possible to avoid finite element based numerical calculations for a unit cell. This, in turn, helps us to obtain efficient and exact closed-form expression of the equivalent elastic moduli of the entire lattice, as explained in the next section.

2.2. Effective elastic moduli of space-filled lattices

The effective elastic moduli of hexagonal honeycomb-like cellular materials without any infill was obtained in published literature [28], as presented in the supplementary material (refer to equations S28 - S32) for ready reference. Our aim in this section is to obtain similar closed-form expressions when the lattices is filled with an elastic material. In the preceding section, we have derived the element stiffness matrices for a single beam with the equivalent effect of space-filling based on two different methods (exact element stiffness and conventional stiffness). From these stiffness matrices, analytical expressions of the in-plane elastic moduli are obtained in this section (refer to figure S1 in the supplementary material for the unit cell deformation mechanics and detailed derivation of the elastic moduli). For the purpose of deriving such expressions concerning space-filled lattices, the element stiffness matrix is re-written in the following general form

$$\mathbf{D}_e = [A_{ij}]_{4\times 4} \tag{5}$$

where $i, j = 1, 2, 3, 4$. Terms of the above matrix have the expressions corresponding to equation (3) (for exact element stiffness matrix) and equation (2) (for conventional stiffness matrix).

2.2.1. Young's modulus E_1

Effective Young's modulus E_1 of the space-filled lattice can be explicitly expressed in terms of the A_{33} element of the stiffness matrix as (refer to the supplementary material section S2.1 for detailed derivation)

$$E_1 = \frac{A_{33} l \cos\theta}{(h + l\sin\theta)\bar{b}\sin^2\theta} \tag{6}$$

If the conventional element stiffness matrix is used, the expression of A_{33}, in view of equation (5), can be obtained from equation (2) as

$$A_{33} = \frac{12EI}{l^3} + \frac{13kl}{35} \tag{7}$$

On the other hand, if the transcendental stiffness matrix is used, the expression of A_{33} can be obtained from equation (3) as

$$A_{33} = \frac{2EIb}{(S^2 - s^2)} 2\,b^2\,(SC + sc) = \frac{4EIb^3\,(SC + sc)}{(S^2 - s^2)} \tag{8}$$

Replacing the expression for A_{33} and $I = \dfrac{\bar{b}t^3}{12}$, the Young's modulus E_1 while using the conventional stiffness matrix can be obtained as

$$\begin{aligned} E_1 &= \frac{A_{33} l\cos\theta}{(h + l\sin\theta)\bar{b}\sin^2\theta} = \frac{A_{33}}{\bar{b}} \frac{\cos\theta}{(\frac{h}{l} + \sin\theta)\sin^2\theta} \\ &= \left(E\left(\frac{t}{\bar{l}}\right)^3 + \underbrace{k\left(\frac{13}{35}\right)\left(\frac{l}{\bar{b}}\right)}_{\text{contribution of filler stiffness}} \right) \frac{\cos\theta}{(\frac{h}{l} + \sin\theta)\sin^2\theta} \end{aligned} \tag{9}$$

Here E is the intrinsic elastic modulus of the honeycomb material and t is the thickness of honeycomb cell wall. In the absence of the elastic filler, we have $k = 0$. In that case, the above expression reduces to the exactly same expression given by Gibson and Ashby [28].

Replacing the expression for A_{33} using the transcendental stiffness matrix and $I = \dfrac{\bar{b}t^3}{12}$, the Young's modulus E_1 can be obtained as

$$\begin{aligned} E_1 = \frac{\sigma_1}{\epsilon_{11}} &= \frac{A_{33}}{\bar{b}} \frac{\cos\theta}{(\frac{h}{l} + \sin\theta)\sin^2\theta} \\ &= \frac{E(bt)^3\,(\sinh(bl)\cosh(bl) + \sin(bl)\cos(bl))}{3\left(\sinh^2(bl) - \sin^2(bl)\right)} \frac{\cos\theta}{(\frac{h}{l} + \sin\theta)\sin^2\theta} \end{aligned} \tag{10}$$

It is useful to establish a direct relationship between two expressions of E_1 given by equations (9) and (10). Substituting the value of b and expanding A_{33} (Equation 8) in Taylor series about $k = 0$ we have

$$A_{33} = \frac{4EIb^3\,(SC + sc)}{(S^2 - s^2)} = 12\,\frac{EI}{l^3} + \frac{13}{35}\,lk - \frac{59}{161700}\,\frac{l^5k^2}{EI} + \frac{551}{794593800}\,\frac{l^9k^3}{EI^2} + O(k^4) + \cdots \quad (11)$$

Substituting this expansion in equation (10) and reorganizing different terms, we have the Young's modulus E_1 in a series form

$$E_1 = \left(E\left(\frac{t}{l}\right)^3 + k\left(\frac{13}{35}\right)\left(\frac{l}{\bar{b}}\right) - k\frac{59}{13475}\left(\frac{t}{l}\right)^3\left(\frac{l}{\bar{b}}\right)^2\left(\frac{k}{E}\right) \right.$$
$$\left. + k\frac{1102}{11036025}\left(\frac{t}{l}\right)^6\left(\frac{l}{\bar{b}}\right)^3\left(\frac{k}{E}\right)^2 + O\left(\frac{k}{E}\right)^3 + \cdots \right) \frac{\cos\theta}{(\frac{h}{l} + \sin\theta)\sin^2\theta} \quad (12)$$

The first two terms of this series is exactly the same as obtained in equation (9) using the conventional stiffness matrix. The higher-order terms in the above expression depend on the non-dimensional ratios $\frac{t}{l}$, $\frac{l}{\bar{b}}$ and $\frac{k}{E}$. In particular, if the value of the filler stiffness k becomes comparatively higher with respect to the elastic modulus of the honeycomb material E, the higher-order terms could be significant. Therefore, equation (10) naturally takes into account all possible values the filler stiffness, while equation (9) can be viewed as a two-term approximation. Finally, it can be noted that the classical result of Gibson and Ashby [28] without the filler stiffness is the one-term approximation of the series in equation (12).

In order to obtain physical insights from the expressions, it useful to view the results in terms of non-dimensional parameters describing the system. We introduce geometric non-dimensional ratios α, η and γ as

$$\alpha = \frac{t}{l}, \quad \eta = \frac{h}{l} \quad \text{and} \quad \gamma = \frac{\bar{b}}{l} \quad (13)$$

For the stiffness of the filler material, the following non-dimensional ratio has been introduced

$$\kappa = \frac{k}{E} \quad (14)$$

Using these, for the case of employing the conventional stiffness matrix in equation (2), the equivalent modulus E_1 is obtained by rewriting (9) as

$$E_1 = E\left(\alpha^3 + \frac{13}{35}\frac{\kappa}{\gamma}\right)\frac{\cos\theta}{(\eta + \sin\theta)\sin^2\theta} \quad (15)$$

When the transcendental stiffness matrix is used, the necessary coefficients are obtained from equation (3). Considering the expression of constant b, we have

$$b = \sqrt[4]{\frac{k}{4EI}} = \sqrt[4]{\frac{\kappa E}{4E\bar{b}t^3/12}} = \frac{1}{l}\sqrt[4]{\frac{3\kappa}{\gamma\alpha^3}} = \frac{\beta}{l} \quad (16)$$

where the non-dimensional coefficient

$$\beta = \sqrt[4]{\frac{3\kappa}{\gamma\alpha^3}} \quad (17)$$

Using this, the equivalent modulus E_1 is obtained in terms of non-dimensional variables by rewriting equation (10) as

$$E_1 = \frac{E\alpha^3\cos\theta}{(\eta + \sin\theta)\sin^2\theta}\,\frac{(SC + sc)}{3(S^2 - s^2)} \quad (18)$$

In the above expressions $C = \cosh\beta$, $c = \cos\beta$, $S = \sinh\beta$ and $s = \sin\beta$.

2.2.2. Young's modulus E_2

The effective Young's modulus E_2 can be explicitly expressed in terms of the A_{33} element of the stiffness matrix as (refer to the supplementary material section S2.2 for detailed derivation)

$$E_2 = \frac{A_{33}}{\bar{b}} \frac{(\frac{h}{l} + \sin\theta)}{\cos^3\theta} \tag{19}$$

Similar to the expression of E_1 discussed in the previous subsection, the term $\frac{A_{33}}{\bar{b}}$ appears in the expression of E_2 also. Consequently the final expressions of E_2 can be obtained in a similar manner by substituting the expression A_{33} from the conventional and transcendental stiffness matrix. Therefore, with the conventional stiffness matrix we have

$$E_2 = \left(E \left(\frac{t}{\bar{l}}\right)^3 + k \left(\frac{13}{35}\right) \left(\frac{l}{\bar{\bar{b}}}\right) \right) \frac{(\frac{h}{l} + \sin\theta)}{\cos^3\theta} \tag{20}$$

Replacing the expression for A_{33} using the corresponding element from the transcendental stiffness matrix, the Young's modulus E_2 can be obtained as

$$E_2 = \frac{E(bt)^3 \left(\sinh(bl)\cosh(bl) + \sin(bl)\cos(bl)\right)}{3\left(\sinh^2(bl) - \sin^2(bl)\right)} \frac{(\frac{h}{l} + \sin\theta)}{\cos^3\theta} \tag{21}$$

It may be noted that the above general expressions approach to the classical result of Gibson and Ashby [28] when the filler stiffness $k \to 0$. In general, the comparative perspectives of E_2 obtained based on conventional and transcendental stiffness matrices are similar to the case of E_1. Substituting the expansion of A_{33} from equation (11) in equation (19) and reorganising different terms, we have the Young's modulus E_2 in a series form

$$E_2 = \left(E \left(\frac{t}{\bar{l}}\right)^3 + k \left(\frac{13}{35}\right) \left(\frac{l}{\bar{\bar{b}}}\right) - k\frac{59}{13475} \left(\frac{t}{\bar{l}}\right)^3 \left(\frac{l}{\bar{\bar{b}}}\right)^2 \left(\frac{k}{E}\right) + k\frac{1102}{11036025} \left(\frac{t}{\bar{l}}\right)^6 \left(\frac{l}{\bar{\bar{b}}}\right)^3 \left(\frac{k}{E}\right)^2 + O\left(\frac{k}{E}\right)^3 + \cdots \right) \frac{(\frac{h}{l} + \sin\theta)}{\cos^3\theta} \tag{22}$$

The first two terms of this series is exactly the same as obtained in equation (20) using the conventional stiffness matrix. The higher-order terms in the above expression depend on the non-dimensional ratios $\frac{t}{\bar{l}}$, $\frac{l}{\bar{\bar{b}}}$ and $\frac{k}{E}$. In particular, if the value of the filler stiffness k becomes comparatively higher with respect to the elastic modulus of the honeycomb material E, the higher-order terms could be significant. Therefore, equation (21) naturally takes into account all possible values the filler stiffness, while equation (20) can be viewed as a two-term approximation. Finally, it can be noted that the classical result of Gibson and Ashby [28] without the filler stiffness is the one-term approximation of the series in equation (22).

Following a similar non-dimensional scheme as E_1, the expressions for E_2 can be written considering conventional and transcendental stiffness matrix respectively as

$$E_2 = E \left(\alpha^3 + \frac{13}{35}\frac{\kappa}{\gamma}\right) \frac{(\eta + \sin\theta)}{\cos^3\theta} \tag{23}$$

$$E_2 = \frac{E\alpha^3(\eta + \sin\theta)}{\cos^3\theta} \frac{(SC + sc)}{3(S^2 - s^2)} \tag{24}$$

In the above expressions $C = \cosh\beta$, $c = \cos\beta$, $S = \sinh\beta$ and $s = \sin\beta$.

2.2.3. Poisson's ratios ν_{12} and ν_{21}

We have presented the detailed derivations of the effective Poisson's ratios of the honeycomb lattices in the supplementary material (refer to section S2.3). Expression for Poisson's ratio due to loading in direction 1 can be obtained as

$$\nu_{12} = \frac{\cos^2\theta}{(\eta + \sin\theta)\sin\theta} \tag{25}$$

Similarly the expression for Poisson's ratio due to loading in direction - 2 can be obtained as

$$\nu_{21} = \frac{(\eta + \sin\theta)\sin\theta}{\cos^2\theta} \tag{26}$$

Note here that $\eta = \frac{h}{l}$ is a non-dimensional geometric parameter. From the above expressions, it is evident that Poisson's ratios ν_{12} and ν_{21} are independent the stiffness of the filler material and same as the expressions given by Gibson and Ashby [28]. In this context it is interesting to note that the proposed expressions of the elastic moduli conform the reciprocal theorem as

$$E_1\nu_{21} = E_2\nu_{12} = \frac{A_{33}}{\bar{b}}\frac{1}{\sin\theta\cos\theta} \tag{27}$$

The above equation satisfying the fundamental theories of materials science provides confidence on the presented expressions of effective elastic moduli in this article.

2.2.4. Shear modulus G_{12}

The effective shear modulus of the space-filled honeycomb lattices in terms of the general beam stiffness matrix elements can be expressed as (refer to the supplementary material section S2.4 for detailed derivation)

$$G_{12} = \frac{(\frac{h}{l} + \sin\theta)}{\bar{b}\cos\theta}\frac{1}{\left(\frac{h^2}{2lA^s_{43}} + \frac{4A^v_{44}}{A^v_{44}A^v_{33} - (A^v_{34})^2}\right)} \tag{28}$$

We will utilise this expression to obtain shear modulus in terms of the geometric and intrinsic material parameters for the case of conventional and transcendental stiffness matrices.

It can be noted that four elements from two different stiffness matrices are necessary here. The conventional stiffness matrix given in equation (2) is considered first. The coefficient of the element stiffness matrix of the slant member is A^s_{43}. We also need other elements of the stiffness matrix of the vertical member (indicated using superscript v) with half the length. Therefore, the four coefficients are given by

$$\begin{aligned} A^s_{43} = -6\frac{EI}{l^2} - \frac{11}{210}kl^2, A^v_{33} = \frac{12EI}{(h/2)^3} + k\frac{13}{35}(h/2), \\ A^v_{34} = -\frac{6EI}{(h/2)^2} - k\frac{11}{210}(h/2)^2, A^v_{44} = \frac{4EI}{(h/2)} + k\frac{1}{105}(h/2)^3 \end{aligned} \tag{29}$$

Closed-form expression of G_{12} can be obtained by substituting these expressions in equation (28)

$$G_{12} = \frac{\frac{E\alpha^3}{\eta^2}\frac{(\eta+\sin\theta)}{\cos\theta}}{\left(\frac{105\,\gamma}{105\,\gamma + 11\,\frac{\kappa}{\alpha^3}} + \frac{96\,\eta^5\gamma\,\kappa + 53760\,\alpha^3\eta\,\gamma^2}{\frac{\eta^8\kappa^2}{\alpha^3} + 1632\,\eta^4\gamma\,\kappa + 26880\,\alpha^3\gamma^2}\right)} \tag{30}$$

where $\alpha = \frac{t}{l}$, $\eta = \frac{h}{l}$, $\gamma = \frac{\bar{b}}{l}$ and $\kappa = \frac{k}{E}$ are non-dimensional geometric and material parameters.

When the transcendental stiffness matrix is used, the necessary coefficients are obtained from equation (3). Considering the appropriate lengths, we have

$$\begin{aligned} A^v_{33} &= \frac{4EIb^3}{(S^{v^2}-s^{v^2})}\left(S^vC^v+s^vc^v\right), A^s_{43} = -\frac{2EIb^2}{(S^2-s^2)}\left(C^2-c^2\right), \\ A^v_{34} &= -\frac{2EIb^2}{(S^{v^2}-s^{v^2})}\left(C^{v^2}-c^{v^2}\right), A^v_{44} = \frac{2EIb}{(S^{v^2}-s^{v^2})}(S^vC^v-s^vc^v) \end{aligned} \tag{31}$$

where $C^v = \cosh\left(\frac{bh}{2}\right)$ $c^v = \cos\left(\frac{bh}{2}\right)$ $S^v = \sinh\left(\frac{bh}{2}\right)$ and $s^v = \sin\left(\frac{bh}{2}\right)$. The parameter $b = \sqrt[4]{\frac{k}{4EI}}$ can be obtained as before. Using the coefficients from equation (31), the expression of G_{12} can be obtained after some algebraic simplifications as

$$G_{12} = \frac{\frac{E\alpha^3}{\eta^2}\frac{(\eta+\sin\theta)}{\cos\theta}}{\left(\frac{3\,C^2+3\,c^2-6}{C^2\beta^2-\beta^2c^2} - \frac{24(-S^vC^v+s^vc^v)\left((C^v)^2+(c^v)^2-2\right)}{\left((c^v)^4+\left(2\,(C^v)^2-2\right)(c^v)^2-(C^v)^4+2\,(S^v)^2(C^v)^2\right)\beta^3\eta^2}\right)} \tag{32}$$

In the above expressions $C = \cosh\beta$, $c = \cos\beta$, $S = \sinh\beta$, $s = \sin\beta$ and $C^v = \cosh(\beta\eta/2)$ $c^v = \cos(\beta\eta/2)$ $S^v = \sinh(\beta\eta/2)$ and $s^v = \sin(\beta\eta/2)$.

Based on the analytical derivation presented in this section, for convenience of the readers, the closed-from expressions obtained using conventional element stiffness matrix and exact element stiffness matrix for space-filled hexagonal lattices are summarized in Table 1 (refer to equations (15) and (18), (23) and (24), (25) and (26), and (30) and (32)). It may be noted in this context that the entire constitutive matrix of a 2D material with honeycomb-like microstructure could be obtained based on the five in-plane elastic moduli reported in this article.

Table 1: Closed-form expressions of effective in-plane elastic moduli for space-filled lattices obtained on the basis of conventional element stiffness matrix (CESM) and exact element stiffness matrix (EESM), as presented in equations 2 and 3 respectively. Note that these expressions can be reduced to the formulation for hexagonal lattices without any infill as a special case (refer to the supplementary material section S2) [28].

Moduli	Method	Closed-form expression
E_1	CESM	$E_1 = E\left(\alpha^3+\frac{13}{35}\frac{\kappa}{\gamma}\right)\frac{\cos\theta}{(\eta+\sin\theta)\sin^2\theta}$
	EESM	$E_1 = \frac{E\alpha^3\cos\theta}{(\eta+\sin\theta)\sin^2\theta}\frac{(SC+sc)}{3\,(S^2-s^2)}$
E_2	CESM	$E_2 = E\left(\alpha^3+\frac{13}{35}\frac{\kappa}{\gamma}\right)\frac{\eta+\sin\theta}{\cos^3\theta}$
	EESM	$E_2 = \frac{E\alpha^3(\eta+\sin\theta)}{\cos^3\theta}\frac{(SC+sc)}{3\,(S^2-s^2)}$
G_{12}	CESM	$G_{12} = \frac{\frac{E\alpha^3}{\eta^2}\frac{(\eta+\sin\theta)}{\cos\theta}}{\left(\frac{105\,\gamma}{105\,\gamma+11\,\frac{\kappa}{\alpha^3}}+\frac{96\,\eta^5\gamma\,\kappa+53760\,\alpha^3\eta\,\gamma^2}{\frac{\eta^8\kappa^2}{\alpha^3}+1632\,\eta^4\gamma\,\kappa+26880\,\alpha^3\gamma^2}\right)}$
	EESM	$G_{12} = \frac{\frac{E\alpha^3}{\eta^2}\frac{(\eta+\sin\theta)}{\cos\theta}}{\left(\frac{3\,C^2+3\,c^2-6}{C^2\beta^2-\beta^2c^2}-\frac{24(-S^vC^v+s^vc^v)((C^v)^2+(c^v)^2-2)}{((c^v)^4+(2\,(C^v)^2-2)(c^v)^2-(C^v)^4+2\,(S^v)^2(C^v)^2)\beta^3\eta^2}\right)}$
$\nu_{12} = \frac{1}{\nu_{21}}$	CESM	$\nu_{12} = \frac{\cos^2\theta}{(\eta+\sin\theta)\sin\theta}$
	EESM	$\nu_{12} = \frac{\cos^2\theta}{(\eta+\sin\theta)\sin\theta}$

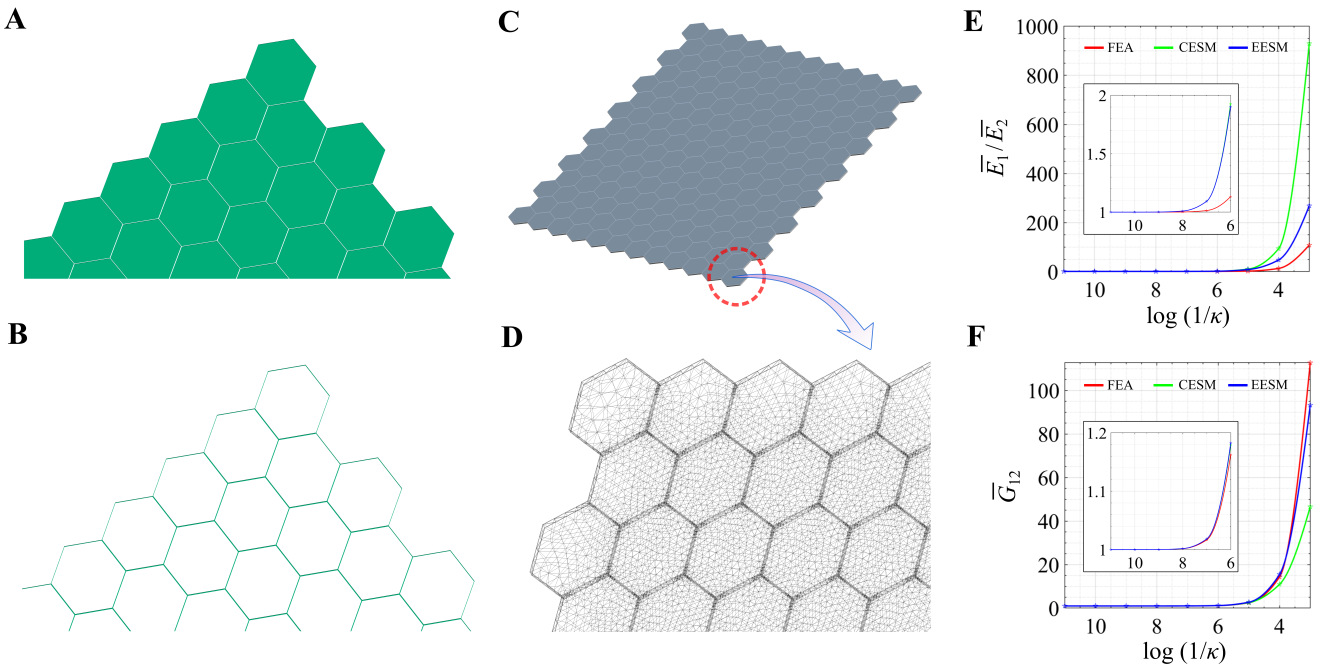

Figure 2: Finite element analysis of filled honeycombs and validation. (A, B) The infill spaces are shown in (A), which are designed to fit inside the void spaces of the lattice frame shown in (B). **(C)** Finite element model of filled honeycomb. Lattice structure embedded in the infill has been modelled for analysis. **(D)** Finite element meshing of the filled honeycomb model. **(E)** Validation results for Young's moduli ratios ($\overline{E_1} = E_1/E_{1_{\mathrm{GA}}}, \overline{E_1} = E_1/E_{1_{\mathrm{GA}}}$) considering loading along direction 1 and 2 (note that the non-dimensional results are same for both the Young's moduli). **(F)** Validation results for shear modulus ratio ($\overline{G_{12}} = G_{12}/G_{12_{\mathrm{GA}}}$) considering loading in the 12 plane. It is to be noted, for validation we have used moduli ratios of the filled honeycomb model with that of the conventional honeycomb model without infill (indicated by the subscript GA).

3. Finite element analysis

The proposed analytical formulae for space-filled lattices (refer to Table 1) are validated with separate finite element simulations. We have developed a finite element model in ANSYS for the filled honeycomb structure with a 12×15 lattice. The number of unit cells is decided based on a convergence study. We have used a cell wall angle of $30°$ and have considered the height to length ratio of the unit cell, $\eta = 1$. For the model, the length, l is considered as 10 mm, infill thickness, $\bar{b}$ as 1 mm and the thickness by length ratio of the beam element, α as 0.02. After modelling, proper bonded connections of the infill material have been established with the corresponding lattice members. Fine meshing has been adopted that creates approximately 231115 tetrahedral elements over an average total surface of 44.061 mm^2 spanning over the infill bodies and the overall lattice as a whole (refer to subfigures (A) and (B) of figure 2). More elements have been considered at the joints considering contact sizing of the connections. The structural model and finite element meshing are shown in subfigures (C) and (D) of figure 2. Keeping the geometrical properties same and the intrinsic Young's modulus of the lattice as 200 GPa, we have varied the Young's modulus of the infill material in orders of 10. It can be noted that the mathematical section provides equations with non dimensional parameters. Using finite element, we have verified that changing the scale of the model uniformly does not bring variation to the results, showing good consistency and stability in our formulation. It is to be noted that we have not used a large deflection solver, however program controlled non-linear analysis method is followed. To check the Young's modulus of the filled honeycomb model along direction 1, we fix the degree of freedoms along direction 1 for the nodes along the extreme left edge whose normal is parallel to direction 1 and apply the loading uniformly over the nodes at the extreme right edge in direction 1. For calculation of the Young's modulus of the filled honeycomb model along direction 2, we fix the degree of freedoms along direction 2 for the nodes along the extreme bottom edge whose normal is parallel to direction

2 and apply the loading uniformly over the nodes at the extreme top edge in direction 2. For the shear modulus of the filled honeycomb model in the 12 plane, we fix the degree of freedoms both along direction 1 and 2 for the nodes along the extreme bottom edge whose normal is parallel to direction 2 and apply the loading uniformly over the nodes at the extreme top edge in direction 1. The rotational degrees of freedom at the edges are not constrained in any of the three cases. Different components of strains as per the basic definitions of elastic moduli are calculated based on the deformation of the lattice under respective applied loads. The corresponding stress values are calculated from the applied edge loads. Subsequently, the elastic moduli are evaluated based on the stress and strain values under small deformation.

In this validation section, we have compared the Young's and shear moduli of the filled honeycomb that we get from finite element analysis with that of the analytical formulation results. It is shown in subfigures (E) and (F) of figure 2 that upto an order of 10^6 of the infill's Young's modulus, our results match quite well. Outside this range, the mechanics of deformation involves other modes that are beyond the scope of current the analytical model. We further note that the results are more accurate with respect to finite element simulations when we use the exact element stiffness matrix formulation (EESM) compared to the conventional element stiffness matrix formulation (CESM). This is expected as explained in the preceding section, particularly when the filler stiffness becomes higher.

4. Results and discussion

In the previous section, we have noted that the in-plane Poisson's ratios remain unaffected by the inclusion of filler material. For the sake of completeness variations of Poisson's ratios are shown in the supplementary material considering auxetic and non-auxetic configurations (refer to figure S4). The feasibility of manufacturing the auxetic structures ($h/l \geq 2\sin\theta$) is taken into account while presenting the results. We concentrate on the two Young's moduli and the shear modulus for presenting numerical results in the following paragraphs. To accentuate the effect of filler material, the results are presented in non-dimensional forms. Though such numerical results are applicable to different cell angles with auxetic and non-auxetic configurations, one should keep in mind the geometric feasibility for manufacturing as discussed above.

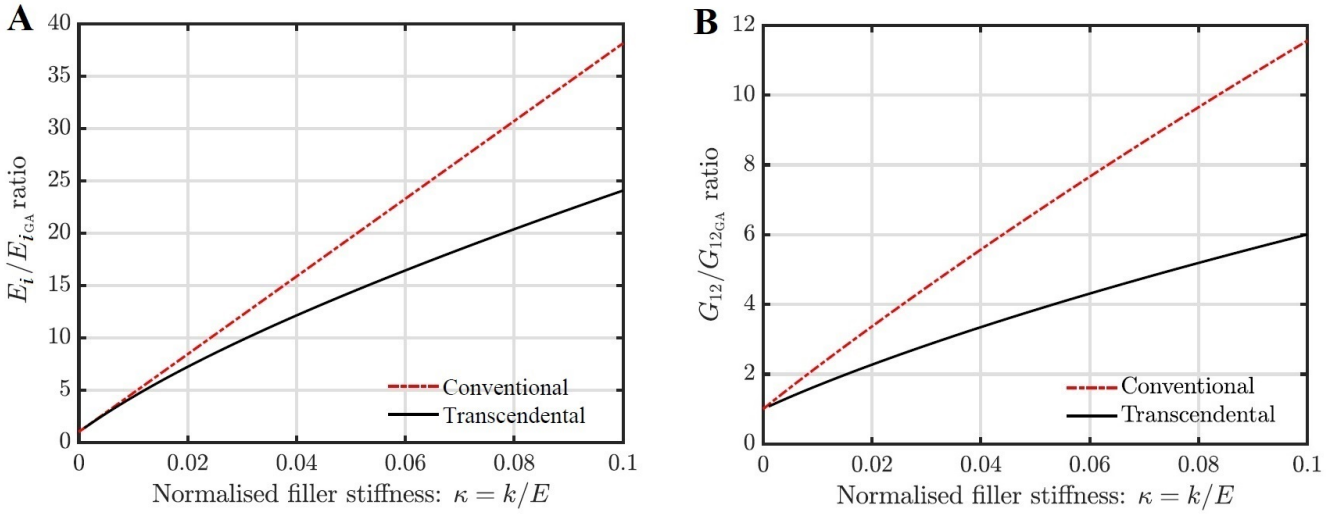

Figure 3: Normalised effective elastic moduli of space-filled lattices obtained using conventional stiffness matrix and transcendental stiffness matrix. **(A)** Normalised Young's modulus $E_i/E_{i_{\mathrm{GA}}}$, where $i = 1, 2$. Note that although the expressions of E_1 and E_2 are different, the ratios $E_1/E_{1_{\mathrm{GA}}}$ and $E_2/E_{2_{\mathrm{GA}}}$ are the same. Thus we present only one plot that represents the results of both the Young's moduli. The actual value of the two Young's moduli, which are different, can be obtained by multiplying the presented numerical values by the corresponding Young's modulus of unfilled lattices. **(B)** Normalised shear modulus $G_{12}/G_{12_{\mathrm{GA}}}$. For generality, here the results are plotted as functions of $\kappa = k/E$ for a value of $\eta = h/l = 1$, $\alpha = t/l = 0.1$ and $\gamma = \bar{b}/l = 1$. The subscript GA is used to indicate the elastic moduli obtained based on the case of unfilled honeycomb lattices [28].

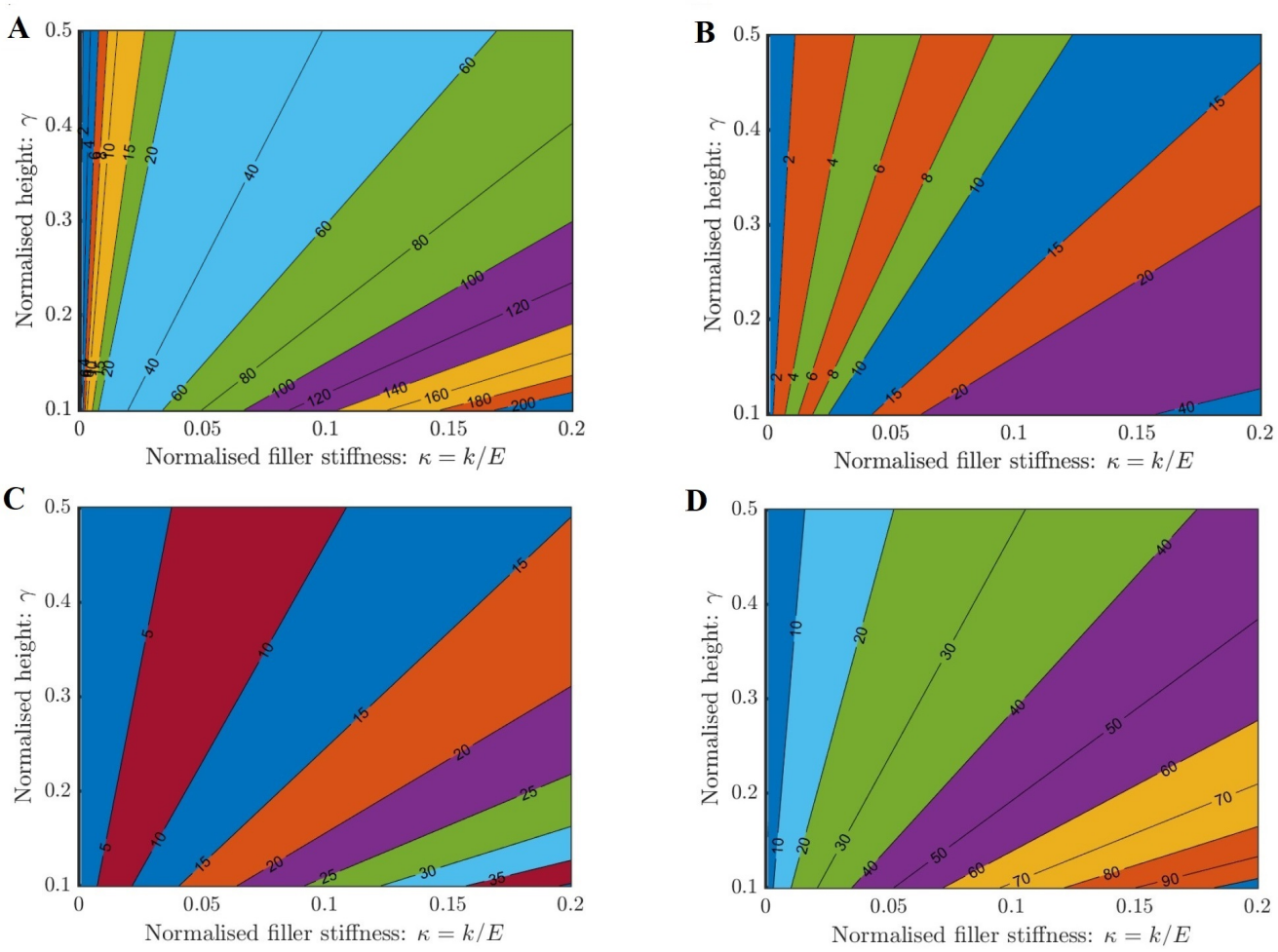

Figure 4: The interaction effect of filler stiffness and height ratios on the in-plane elastic moduli. Normalised Young's moduli $E_i/E_{i_{\mathrm{GA}}}$ (where $i = 1, 2$) and normalised shear modulus $G_{12}/G_{12_{\mathrm{GA}}}$ are plotted as a function of the filler stiffness ratio $\kappa = k/E$ and the height ratio $\gamma = \bar{b}/l$. Two values of the thickness ratio $\alpha = 0.1$ and 0.2 are considered. The subscript GA is used to indicate the elastic moduli obtained based on the case of unfilled honeycomb lattices [28]. Note that although the expressions of E_1 and E_2 are different, the ratios $E_1/E_{1_{\mathrm{GA}}}$ and $E_2/E_{2_{\mathrm{GA}}}$ are the same and these two non-dimensional quantities are independent of η. Thus we present only one plot that represents the results of both the Young's moduli. The actual value of the two Young's moduli, which are different, can be obtained by multiplying the presented numerical values by the corresponding Young's modulus of unfilled lattices (refer to the supplementary material section S2 where closed form expressions are provided for the effective Young's modulus of unfilled lattices). **(A)** Young's modulus with $\alpha = 0.1$ **(B)** Young's modulus with $\alpha = 0.2$ **(C)** Shear modulus with microstructural configuration: $\eta = 1$, $\alpha = 0.1$ **(D)** Shear modulus with microstructural configuration: $\eta = 2$, $\alpha = 0.1$.

From the expressions of E_1, E_2 and G_{12} obtained in terms of non-dimensional geometrical and material parameters following the conventional and transcendental stiffness matrix (refer to Table 1), it can be verified that when the filler material is not present (by taking the limit $\kappa \to 0$), the expressions reduce to the classical expressions provided in literature by Gibson and Ashby [28]. Along with the detailed finite element validation presented in the preceding section, this renders an exact analytical validation of the proposed derivations as a special case. Further confidence on the developed formulation can be obtained by comparing the numerical results from the conventional and transcendental stiffness matrices. In the preceding section, it is shown that the elastic moduli obtained using transcendental stiffness matrices are more accurate, while the formulation based on conventional stiffness matrix is valid only for relatively lesser stiffness of the filler material. Thus, the elastic moduli obtained using the two approaches are expected to match only for a low stiffness of the filler material. This aspect will be more evident from the numerical results presented later in this section.

In order to compare both the approaches, in figure 3, Young's moduli (E_1 and E_2) and shear

modulus (G_{12}) are shown as functions of $\kappa = k/E$. The values in the Y-axis are normalised with respect to the equivalent classical results without any filler [28] (the equations of five in-plane elastic moduli are presented in supplementary material section S2), as indicated by subscripts GA. Although the expressions of E_1 and E_2 are different, the ratios $E_1/E_{1_{\mathrm{GA}}}$ and $E_2/E_{2_{\mathrm{GA}}}$ are the same. Therefore, only E_i (where $i = 1, 2$) is considered in figure 3. The parameters used in figure 3 are $\eta = h/l = 1$, $\alpha = t/l = 0.1$ and $\gamma = \bar{b}/l = 1$. As explained before, it can be observed that the results obtained using the conventional stiffness matrix is accurate only for very small values of κ. This demonstrates the advantage of using the proposed approach with the transcendental stiffness matrix. The closed-form expressions in equation (18), (24) and (32) are exact and therefore valid for higher values of the filler stiffness. In figure 3, significant increase in the effective moduli is observed. Such enhancement can have a potential impact on engineering applications. This motivates us to study how the effective moduli increase as different parameters in the model change.

In figure 4(A-B), contours of normalised Young's moduli $E_i/E_{i_{\mathrm{GA}}}$ are plotted as a function of the filler stiffness ratio κ and the height ratio γ. Two values of the thickness ratio, namely, $\alpha = 0.1$ and 0.2 are shown, wherein it can be noticed that when the cell walls are thinner, the infill has more influence on the equivalent Young's modulus (note that $E_i/E_{i_{\mathrm{GA}}}$ for $i = 1, 2$ are independent of η). For an infill stiffness of only 10%, it is possible to increase the equivalent Young's modulus by an order of magnitude. This is encouraging as lightweight elastic foams can be used as an infill to substantially increase Young's modulus. Closed-form formulae derived in this paper can be used to design such composite 2D lattices efficiently.

Contours of normalised shear modulus $G_{12}/G_{12_{\mathrm{GA}}}$ are plotted as a function of the filler stiffness ratio κ and the height ratio γ in figure 4(C-D). Two values of η, namely $\eta = h/l = 1, 2$ are considered. The normalised shear modulus increase with η. The pattern of change with respect to the other parameters remain similar to the case of E_1 and E_2. Again we note that orders of magnitude of increase in the shear modulus is possible with the inclusion of the filler material. Further numerical results for the Young's moduli and shear modulus to investigate the effects of α and η are presented in the supplementary material (refer to figures S2 and S3). In general, the numerical outcomes demonstrate that the developed analytical framework for the elastic moduli could be utilised for efficiently designing space-filled lattices to simultaneously possess different values of the elastic moduli by identifying the appropriate microstructures. Such explicit modulation of stiffness corresponding to longitudinal, transverse and shear modes would facilitate the development of engineered microstructures with programmable direction-dependent dynamic properties. The closed-form formulae would also act as a ready reference to characterise the structural viability of different mechanical and biological systems (naturally occurring and artificial) and multi-functional devices where filled-honeycombs are present.

5. Conclusions and perspective

An analytical framework leading to closed-form formulae for the effective in-plane elastic moduli of space-filled hexagonal lattices is proposed. In general, the elastic properties of lattice-like honeycomb structures have received tremendous attention from the scientific community over the last few decades. Traditionally such lattices are made of a network of beams in two and three dimensions with majority of the volume of the lattice structures being void space. Recently researchers have started exploring ways to utilise this void space for multi-functional property modulation of lattices. For example, if we could have a filled multi-material lattice structure, the global mechanical behaviour including different elastic moduli, wave propagation, vibration, impact and acoustic features can be simultaneously modulated in a substantially expanded design space with additional parameters related to the stiffness, mass and damping of the filler, leading to exciting multi-functional properties. However, the effective elastic moduli are always of crucial importance to ensure the structural viability of various multi-functional devices and systems where a space-filled lattice material could potentially be used. Here we have developed analytical

expressions for the effective in-plane elastic moduli of such space-filled lattices based on an exact element stiffness matrix approach coupled with the unit cell method, wherein the transcendental shape functions are used to satisfy the equilibrium at all points of the structural domain. The transcendental functions are obtained from the exact solution of the underlying differential equations with appropriate displacement boundary conditions. For establishing the analytical model we have proposed a mechanical equivalence of space-filled lattices with equivalent networks of beam elements. The numerical results are compared with the elastic moduli obtained from traditional stiffness matrices, wherein a good agreement is found for relatively lesser value of the filler stiffness. The proposed expressions of the elastic moduli converge to the classical closed-form expressions provided in the scientific literature when the stiffness of the filler material tends to zero, leading to an exact analytical validation as a special case. Further, separate finite element simulations are carried out to validate the closed form expressions of space-filled lattices. From the derived analytical expressions, it becomes evident that the two Poisson's ratios are not affected by the presence of filler material, while two Young's moduli and the shear modulus can be modulated significantly depending on the filler stiffness. The physics-based analytical formulae reveal that elastic properties of the space-filled lattice depend on the thickness of the lattice sheet unlike the case of conventional honeycombs without any filler material.

From the perspective of engineered material microstructures, the present investigation introduces a new dimension in terms of the properties of filler material for simultaneously modulating multi-physical mechanical behaviour of lattice materials. The scope of explicit modulation of stiffness corresponding to longitudinal, transverse and shear modes, besides rendering the possibility of designing application-specific multi-objective static deformation behaviour, would facilitate the development of engineered microstructures with programmable direction-dependent dynamic and wave propagation properties. The numerical results show that the inclusion of filler material with even a relatively lower stiffness value (normalised filler stiffness $\sim$0.1) can lead to an increase in the effective elastic moduli up to few orders of magnitude. This effect can potentially be exploited in the design of novel space-filled composite lattices for having higher global stiffness and simultaneously modulating different in-plane normal and shear components. The efficient analytical framework will also act as a ready reference to characterise the structural viability of different mechanical and biological systems (naturally occurring and artificial) and multi-functional devices where filled honeycombs are present.

The proposed analytical formulae will have an impact both in the forward (for readily characterising different components of the stiffness of a filled lattice designed for other multi-functional applications or already in existence) and inverse analyses (for identifying the lattice microstructure in a significantly expanded design space to achieve multi-objective goals related to possessing an adequate level of multiple elastic moduli with the possibility of significantly enhancing them) of lattice-like systems across the length-scales. Even though here we have concentrated on the analysis of hexagonal lattices, the disseminated concepts (including the general methodology of derivation and numerical results) can be extended to other forms of beam-based lattices and metamaterials with two and three dimensional structural forms. Such closed-form analytical expressions provide a computationally efficient paradigm to investigate the system in intricate details and with adequate level of physical insights, leading to the scope of material innovation without the practical hindrance of computational or experimental expenses and time. This will be particularly appealing for innovating next-generation of application-specific multi-functional material microstructures where thousands of realisations are required to be analysed due to the involvement of inverse identification algorithms based on multi-objective optimisation.

Acknowledgments

TM and SN acknowledge the initiation grant received from University of Southampton.

References

[1] Fleck, N. A., Deshpande, V. S., Ashby, M. F., 2010. Micro-architectured materials: past, present and future. Proceedings of the Royal Society of London A: Mathematical, Physical and Engineering Sciences 466 (2121), 2495–2516.

[2] Sinha, P., Mukhopadhyay, T., 2023. Programmable multi-physical mechanics of mechanical metamaterials. Materials Science & Engineering R (In press).

[3] Zhang, J., Lu, G., You, Z., 2020. Large deformation and energy absorption of additively manufactured auxetic materials and structures: A review Composites Part B: Engineering, 201, 108340.

[4] Cummer, S. A., Christensen, J., Alù, A., 2016. Controlling sound with acoustic metamaterials. Nature Reviews Materials 1 (3), 16001.

[5] Lai, Y., Wu, Y., Sheng, P., Zhang, Z.-Q., 2011. Hybrid elastic solids. Nature materials 10 (8), 620.

[6] Khakalo S., Balobanov V., Niiranen J., 2019. Modelling size-dependent bending, buckling and vibrations of 2D triangular lattices by strain gradient elasticity models: Applications to sandwich beams and auxetics. International Journal of Engineering Science 127 33 - 52.

[7] Chen Y., Hu H., 2020. In-plane elasticity of regular hexagonal honeycombs with three different joints: A comparative study: Mechanics of Materials, 148 103496.

[8] Mukhopadhyay, T., Adhikari, S., 2017. Stochastic mechanics of metamaterials. Composite Structures 162, 85 – 97.

[9] Mukhopadhyay T, Adhikari S. 2016 Effective in-plane elastic properties of auxetic honeycombs with spatial irregularity. *Mechanics of Materials* **95**, 204 – 222.

[10] Mukhopadhyay T, Naskar, S, Adhikari S. 2020 Anisotropy tailoring in geometrically isotropic multi-material lattices. Extreme Mechanics Letters, 40, 100934.

[11] Li, J., Chan, C. T., 2004. Double-negative acoustic metamaterial. Phys. Rev. E 70, 055602.

[12] Liu, Z., Zhang, X., Mao, Y., Zhu, Y. Y., Yang, Z., Chan, C. T., Sheng, P., 2000. Locally resonant sonic materials. Science 289 (5485), 1734–1736.

[13] Adhikari S., Mukhopadhyay T., Shaw A., Lavery N.P., 2020. Apparent negative values of Young's moduli of lattice materials under dynamic conditions. International Journal of Engineering Science 150 103231.

[14] Wu, Y., Lai, Y., Zhang, Z.-Q., 2011. Elastic metamaterials with simultaneously negative effective shear modulus and mass density. Phys. Rev. Lett. 107, 105506.

[15] Zheng, L. Y., Zhang, X. J., Lu, M. H., Chen Y. F., Christensen J., 2021. Knitting topological bands in artificial sonic semimetals. Materials Today Physics, 16, 100299.

[16] Milton, G. W., Briane, M., Willis, J. R., 2006. On cloaking for elasticity and physical equations with a transformation invariant form. New Journal of Physics 8 (10), 248.

[17] Dos Reis, F and Ganghoffer, JF 2012. Construction of micropolar continua from the asymptotic homogenization of beam lattices. Computers & Structures 112 354–363.

[18] Dos Reis, Francisco and Ganghoffer, Jean-François 2014. Homogenized elastoplastic response of repetitive 2D lattice truss materials. Computational materials science 84 145–155.

[19] Willis, John R 2011. Effective constitutive relations for waves in composites and metamaterials. Proceedings of the Royal Society A: Mathematical, Physical and Engineering Sciences 467 1865–1879.

[20] Bordiga, Giovanni and Cabras, Luigi and Piccolroaz, Andrea and Bigoni, Davide 2021. Dynamics of prestressed elastic lattices: homogenization, instabilities, and strain localization. Journal of the Mechanics and Physics of Solids 146 104198.

[21] Kutsenko, AA and Nagy, AJ and Su, X and Shuvalov, AL and Norris, AN 2017. Wave propagation and homogenization in 2d and 3d lattices: A semi-analytical approach. The Quarterly Journal of Mechanics and Applied Mathematics 70 131–151.

[22] Karathanasopoulos, Nikolaos and Dos Reis, F and Hadjidoukas, Panagiotis and Ganghoffer, Jean-Francois 2020. LatticeMech: A discrete mechanics code to compute the effective static properties of 2D metamaterial structures. SoftwareX 11 100446.

[23] Ghuku S., Mukhopadhyay T., 2022. Anti-curvature honeycomb lattices for mode-dependent enhancement of nonlinear elastic properties under large deformation. International Journal of Non-Linear Mechanics 140 103887.

[24] Sinha, P., Mukhopadhyay, T., 2023. On-demand contactless programming of nonlinear elastic moduli in hard magnetic soft beam based broadband active lattice materials. Smart Materials and Structures 32 055021.

[25] Singh A., Mukhopadhyay T., Adhikari S., Bhattacharya B., 2022. Active multi-physical modulation of Poisson's ratios in composite piezoelectric lattices: On-demand sign reversal. Composite Structures 280 114857.

[26] Tiwari, P., Naskar, S., Mukhopadhyay, T., 2023. Programmed Out-of-Plane Curvature to Enhance Multimodal Stiffness of Bending-Dominated Composite Lattices. AIAA Journal 61 (4), 1820-1838.

[27] Nakka R., Harursampath D., Pathan M., Ponnusami S. A., 2022. A computationally efficient approach for generating RVEs of various inclusion/fibre shapes. Composite Structures 25 (12), 105656.

[28] Gibson, L., Ashby, M. F., 1999. Cellular Solids Structure and Properties. Cambridge University Press, Cambridge, UK.

[29] Mukhopadhyay T., Adhikari S., Alu A., 2019. Probing the frequency-dependent elastic moduli of lattice materials. Acta Materialia 165 654-665.

[30] Zschernack C., Wadee M. A., Völlmecke C., 2016. Nonlinear buckling of fibre-reinforced unit cells of lattice materials. Composite Structures 136 217 - 228.

[31] Sinha P., Walker M., Mukhopadhyay T., 2023. Non-invariant elastic moduli of bi-level architected lattice materials through programmed domain discontinuity. Mechanics of Materials (In press).

[32] Kundu D., Ghuku S., Naskar S. Mukhopadhyay T., 2023. Extreme specific stiffness through interactive cellular networks in bi-level micro-topology architected metamaterials. Advanced Engineering Materials 2201407.

[33] Mukhopadhyay, T., Adhikari, S., 2017. Effective in-plane elastic moduli of quasi-random spatially irregular hexagonal lattices. International Journal of Engineering Science 119 142-179.

[34] Alavi, SE and Ganghoffer, JF and Sadighi, M and Nasimsobhan, M and Akbarzadeh, AH 2022. Continualization method of lattice materials and analysis of size effects revisited based on Cosserat models. International Journal of Solids and Structures 254 111894.

[35] Ding H., Zhen Z., Imtiaz H., Guo W., Zhu H., Liu B., 2019. Why are most 2D lattices hexagonal? The stability of 2D lattices predicted by a simple mechanics model. Extreme Mechanics Letters 32, 100507.

[36] Mukhopadhyay, T., Mahata, A., Adhikari, S., Zaeem, M. A., 2017. Effective elastic properties of two dimensional multiplanar hexagonal nanostructures. 2D Materials 4 (2), 025006.

[37] Mukhopadhyay T., Adhikari S., 2016. Free vibration analysis of sandwich panels with randomly irregular honeycomb core. Journal of Engineering Mechanics 142(11) 06016008.

[38] Tancogne-Dejean T. and Mohr D., 2018. Elastically-isotropic elementary cubic lattices composed of tailored hollow beams. Extreme Mechanics Letters 22 13 – 18.

[39] Chen D., Zheng X., 2018. Multi-material additive manufacturing of metamaterials with giant, tailorable negative Poisson's ratios. Scientific reports 8 1–8.

[40] Bandyopadhyay A., Heer B., 2018. Additive manufacturing of multi-material structures. Materials Science and Engineering: R: Reports 129 1 - 16.

[41] Skylar T., 2014. 4D printing: multi-material shape change. Architectural Design 84 116–121.

[42] Kang, D., Park, S., Son, Y., Yeon, S., Kim, S. H., Kim, I., 2019. Multi-lattice inner structures for high-strength and light-weight in metal selective laser melting process. Materials & Design 175, 107786.

[43] Vogiatzis P., Chen S., Wang X., Li T., Lifeng W., 2017. Topology optimization of multi-material negative Poisson's ratio metamaterials using a reconciled level set method. Computer-Aided Design 83 15 - 32.

[44] Liu S., Li F., Peng J., Zhang X., 2023. Universal model describing the negative thermal expansion coefficients of bending-type two-dimensional metamaterials with chiral/anti-chiral structures. Composites Communications 39 101559.

[45] Xu H., Pasini D., 2016. Structurally efficient three-dimensional metamaterials with controllable thermal expansion. Scientific reports 6 34924.

[46] Manohar C, Adhikari S. 1998 Dynamic stiffness of randomly parametered beams. Probabilistic Engineering Mechanics **13**, 39 – 51.

[47] Petyt M. 1998 *Introduction to Finite Element Vibration Analysis*. Cambridge, UK: Cambridge University Press.

[48] Dawe D. 1984 *Matrix and Finite Element Displacement Analysis of Structures*. Oxford, UK: Oxford University Press.